A Case Study of Multidisciplinary Surface Faulting Assessment in the Urbanized Fucino Basin, Italy

Francesco Iezzi[1,2], Paolo Boncio[2,3], Alessio Testa[2], Giuseppe Di Giulio[4], Maurizio Vassallo[4], Fabrizio Cara[5], Giuliano Milana[5], Fabrizio Galadini[5], Biagio Giaccio[6] & Mattia De Luca[3]

[1] Department of Earth Sciences, Environment and Resources (DiSTAR), University Federico II, Naples, Italy.
[2] DiSPUTer, University "G. d' Annunzio" Chieti-Pescara, Chieti, Italy.
[3] Department of Engineering and Geology, University "G. d'Annunzio" Chieti-Pescara, Chieti, Italy.
[4] Istituto Nazionale di Geofisica e Vulcanologia, Sezione di Sismologia e Tettonofisica, L'Aquila, Italy.
[5] Istituto Nazionale di Geofisica e Vulcanologia, Sezione di Sismologia e Tettonofisica, Roma, Italy.
[6] Istituto di Geologia Ambientale e Geoingegneria, CNR, Rome, Italy.

FI, 0000-0001-5628-3335; PB, 0000-0002-4129-5779; GDG, 0000-0002-4097-7102; MV, 0000-0001-8552-6965; FC, 0000-0002-1702-563X; GM, 0000-0002-2775-4924; FG, 0000-0002-3095-4724; BG, 0000-0002-7007-9127; MDL, 0000-0002-3074-1913.

Ital. J. Geosci., Vol. 142, No. 1 (2023), pp. 104-121, 11 figs., https://doi.org/10.3301/IJG.2023.03.

Research article

Corresponding author e-mail: francesco.iezzi@unina.it

Citation: Iezzi F., Boncio P., Testa A., Di Giulio G., Vassallo M., Cara F., Milana G., Galadini F., Giaccio B. & De Luca M. (2023) - A Case Study of Multidisciplinary Surface Faulting Assessment in the Urbanized Fucino Basin, Italy. Ital. J. Geosci., 142(1), 104-121, https://doi.org/10.3301/IJG.2023.03.

Associate Editor: Giulio Viola

Submitted: 29 July 2022
Accepted: 16 November 2022
Published online: 22 November 2022

ABSTRACT

The occurrence of coseismic surface ruptures along fault traces in urbanised areas creates a serious hazard to the vulnerability of man-made manufactures. In order to mitigate such hazard, it is necessary to investigate the geometry, the activity and the capability of faults located close to urbanised areas. This paper presents a case study of the investigation of capable faults within a sensitive area in Italy that is characterized by a high density of population and industrial activities, high levels of seismicity and the presence of faults proven to be capable of rupturing the surface during medium-to-large earthquakes. We focused on the Luco fault (Fucino basin, Central Italy), which previous studies have suggested to cross the industrial district of the town of Avezzano. We present a multidisciplinary approach, consisting of Electrical Resistivity Tomography surveys, continuous-coring boreholes and paleoseismological trenches, aimed at accurately constraining the trace of the Luco fault and documenting the associated fault displacement. This allowed us to constrain the geometry of the Luco fault and to assess the associated fault displacement hazard. We suggest that the proposed methodology represents a pilot study for further investigations of capable faults in the Italian and other similar seismotectonic contexts.

KEY-WORDS: earthquake geology, capable faults, fault displacement hazard, fault zoning, paleoseismology.

INTRODUCTION

Fault displacement hazard (FDH) is the hazard due to the occurrence of coseismic ruptures of the ground surface located along fault traces rupturing during medium-to-large earthquakes (e.g., Youngs et al., 2003; Moss & Ross, 2011; Petersen et al., 2011; Baize et al., 2020; Nurminen et al., 2020; Ferrario & Livio, 2021; IAEA, 2015; 2022). The FDH is therefore strictly connected to the presence of the so-called capable faults, that is faults that have accommodated at least one surface-rupturing earthquake in recent times and have the potential for releasing surface-rupturing earthquakes in the future (IAEA, 2022). The identification of capable faults is fundamental for land use purposes, because coseismic surface ruptures can permanently damage man-made infrastructures (i.e., buildings, factories, dams, etc.) located above or in the surroundings of the fault trace, with severe consequences in terms of human and/or economic losses. For instance, the 6th April 2009 M_w 6.1 L'Aquila earthquake in Central Italy produced surface ruptures along the trace of the Paganica fault, causing a water pipeline crossing the fault to break (Fig. 1a; Boncio et al., 2012). Past coseismic displacements of man-made structures can be studied also from paleoseismological/archaeoseismological studies (e.g., Galadini & Galli, 1996; 1999; Galli & Galadini, 2003; Galli & Naso, 2009; Galli et al., 2022).

Common approaches to mitigate the FDH imposed by capable faults are based on the detailed mapping and zoning of the fault traces. The zoning approach, proposed for the first

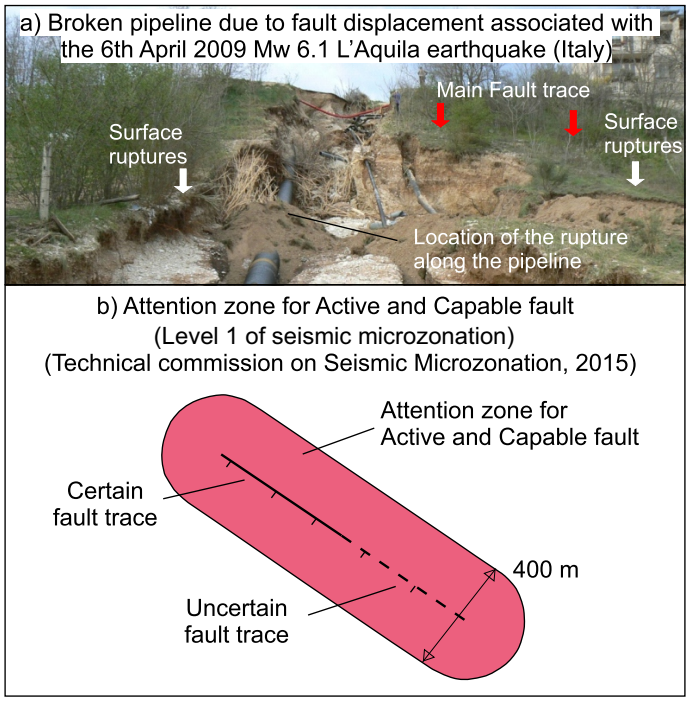

Fig. 1 - a) Example of a broken water pipeline due to surface ruptures produced by the 6th April 2009 M_w 6.1 L'Aquila Earthquake (Italy). b) Zoning approach for the mitigation of fault displacement hazard according to the Italian "Land Use Guidelines for Areas with Active and Capable Faults" (Technical Commission on Seismic Microzonation, 2015). This approach recommends to build an Attention zone (suggested width 400 m) around a fault trace; such zone should be then explored with advanced surveys in order to precisely characterize the active fault (modified after "Land Use Guidelines for Areas with Active and Capable Faults", Technical Commission on Seismic Microzonation, 2015).

time in the Alquist-Priolo Earthquake Fault Zoning Act adopted by the State of California in 1972 (Bryan & Hart, 2007), requires (1) the construction of an Earthquake Fault Zone (EFZ) around the fault trace, defined as the zone where detailed investigations are needed before man-made infrastructures can be built, and (2) the construction of a fault Setback (S) in the proximity of well-defined fault traces, within which no buildings or infrastructures are allowed to be built. Boncio et al. (2012) reviewed the geometry of the EF and S zones for normal faults on the basis of the distribution of coseismic surface ruptures associated with worldwide-distributed normal faulting earthquakes, including also data from the surface ruptures associated with the 2009 M_w 6.1 L'Aquila earthquake in Central Italy. Boncio et al. (2012) suggests to build asymmetric zones around the trace of active normal faults, with the EFZ extending to 150 m in the hanging wall and 30 m in the footwall of the fault trace, and the S 40 m in the hanging wall and 15 m in the footwall. This asymmetric layout reflects the distribution of coseismic ruptures along normal faults: empirical observations have in fact shown that the ruptures are mostly distributed within the hanging wall block of a normal fault (see Boncio et al., 2012, for details). Recently, it has been suggested that the width of fault zones can be variable according to the intrinsic nature of the fault, as in the Special Publication of the California Geological Survey (2018). Moreover, probabilistic approaches are also employed in order to discretise how fault displacement can be distributed along the and across the principal fault trace (e.g., Youngs et al., 2003; Petersen et al., 2011; Nurminen et al., 2020).

In Italy, the Technical Commission on Seismic Microzonation (2015) defines "active and capable faults" in the Italian territory as faults that have released at least one surface-rupturing earthquake in the last 40 kyrs. This time span is longer than common time spans adopted elsewhere (the Holocene, ca. 11,700 ka; California Geological Survey, 2018). The longer time span adopted in Italy is chosen in order to overcome longer earthquake recurrence intervals of active faults (a few thousand years), and also because it represents the time range that can be explored with radiocarbon dating, commonly applied in paleoseismological trenching analysis. In terms of zoning capable faults, the Technical Commission on Seismic Microzonation (2015) suggests to adopt an Attention Zone for active and capable faults (AZ_{ACF}) 400 m wide across the supposed trace of the main surface rupture after having conducted a basic (so called "Level 1") seismic microzonation study. The AZ_{ACF} is defined around active and capable faults already recognised in the literature and should include the uncertainty in the location and geometry of the fault trace and the eventually associated secondary ruptures (Fig. 1b). The AZ_{ACF} has important constraints in urban planning, because it halts the construction of new buildings and infrastructures therein before carrying out specific investigations within the zone. According to the Technical Commission on Seismic Microzonation (2015), specific investigations must be carried out during advanced seismic microzonation studies (so called "Level 3") aimed at (i) defining with certainty the fault trace, around which a 30 m-wide avoidance zone is defined (called Respect Zone); (ii) shaping a Susceptibility Zone where uncertainty remain on fault trace location or possible occurrence of secondary, distributed deformation; and (iii) eventually removing the zone where the study demonstrates absence, inactivity or non-capability of the fault. However, whichever zoning approach is used, it is clear that the first fundamental step for the mitigation of the FDH is the characterization of the fault geometry, its activity and capability of rupturing the surface.

Although in Italy fault displacement represents a serious hazard for many towns and man-made infrastructures close to capable faults (e.g., Testa et al., 2021), the scientific literature presents few studies investigating capable faults localised within already urbanised areas (e.g., Galli et al., 2005; Maceroni et al., 2018; 2022; Galadini et al., 2022). In order to contribute to fill this gap, this paper presents one of the first approaches to investigate capable faults in urban areas in the Italian territory.

Our study is focused within the Fucino basin (Central Apennines, Italy), a region where multiple paleoseismological studies suggested the occurrence of several surface-rupturing earthquakes, with the largest of them causing simultaneous surface ruptures on multiple faults, such as the M_s 7 1915 Avezzano earthquake (Fig. 2; Oddone, 1915; Giraudi, 1986; Michetti et al., 1996; Galadini et al., 1997; 1999; Giraudi, 1998; Galadini & Galli, 1999). We focus in particular on the Luco fault, a E-dipping normal fault that runs on the western flank of the Fucino basin (Fig. 2). Paleoseismological studies have shown that the Luco fault is active and capable of producing surface ruptures

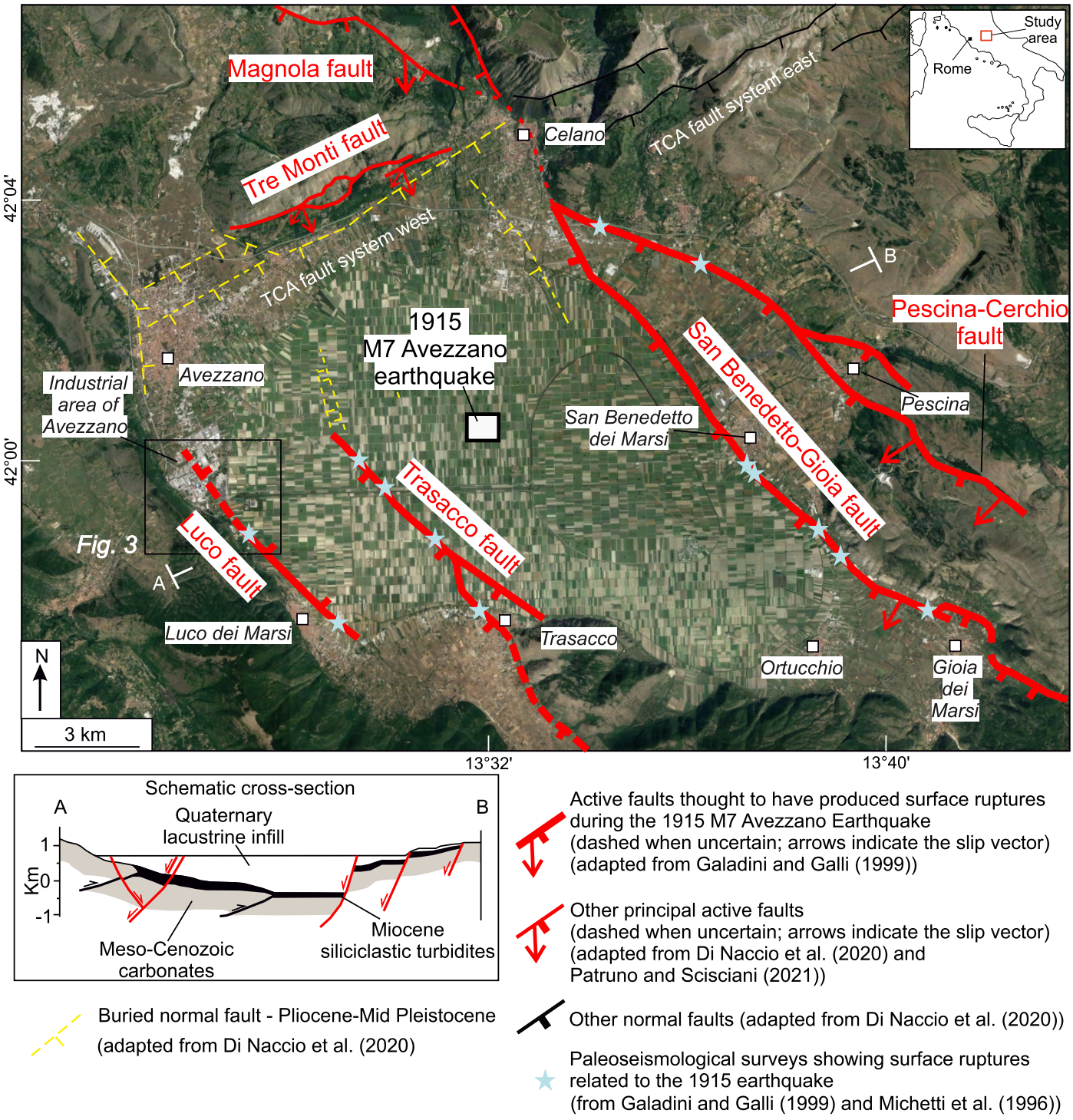

Fig. 2 - Location map of the study area. Thick red traces are active faults thought to have ruptured during the 1915 M 7 Avezzano earthquake (*sensu* Galadini and Galli, 1999); thin red traces are other active faults. Yellow dashed traces are buried normal faults, active during Pliocene-Mid Pleistocene (Di Naccio et al., 2020). Pale blue stars indicate the location of paleoseismological studies showing evidence of surface ruptures associated with the 1915 earthquake (from Michetti et al., 1996, and Galadini & Galli, 1999). In red are the names of the principal active faults. TCA: Tremonti-Celano-Aielli. All the fault traces are modified after Di Naccio et al. (2020), and references therein. Inset cross-section is modified after Cavinato et al. (2002).

(Fig. 2; Giraudi, 1988; Galadini & Galli, 1999; Galli et al., 2016), and for this reason the Luco fault is included in the "ITaly HAzard from CApable faulting" database (ITHACA database; ITHACA Working Group, 2019). Although the fault trace is mostly buried by recent sediments or covered by the product of agricultural activity, and therefore its surface expression is not clear, the local seismic microzonation of the close town of Avezzano (about 42,000 inhabitants) hypothesized that the Luco fault could propagate northward within the industrial district of the town. This has been speculated on the basis of the abrupt deepening of the limestone bedrock shown by two boreholes within the industrial district (the Perrella site in Fig. 3a). Given the capability of the Luco fault, the local Seismic Microzonazion built a AZ_{ACF} around the supposed fault trace (Fig. 3; Di Naccio et al., 2020).

Considering the strategic importance of the industrial district of Avezzano for the local community, we performed a series of investigations along the supposed trace of the Luco fault. We present results obtained through a multi-method approach that integrates geophysical investigations (namely Electrical Resistivity Tomography, ERT), continuous-coring boreholes (wells S1 and S2) and paleoseismological surveys performed in key sites where geological and geophysical data suggested the likely occurrence of faulting close to the ground surface (Fig. 3a). The results are discussed both in terms of the local specific interest of FDH assessment and, more importantly, in a wider methodological perspective of mitigation of FDH, urban planning and zoning of capable faults.

GEOLOGICAL BACKGROUND

The Central Apennines are a Miocene-Early Pliocene fold-and-thrust belt, which has been subsequently dissected by Late Pliocene-Quaternary extensional tectonics that caused the onset of multiple active normal faults striking overall NW-SE (Lavecchia et al., 1994; Patacca et al., 2008). These normal faults caused the formation of several intramountain tectonic depressions, such as the Fucino basin (Fig. 2). The opening and development of the Fucino basin was driven by two different normal fault sets: (i) the first set strikes WSW-ENE, dips towards SSE and it is considered to have played an important role during the early stages of the opening of the Fucino basin in the Late Pliocene-Lower Pleistocene (Tre Monti Fault in Fig. 2; e.g., Cavinato et al., 2002); (ii) the second set took over since Lower/Middle Pleistocene, it strikes NW–SE, dips to the SW and hosts the seismogenic Fucino fault system (Mt. Parasano-Marsicana Highway fault, San Benedetto-Gioia dei Marsi fault) and their synthetic and antithetic faults (Trasacco and Luco faults, respectively; Fig. 2) (Lavecchia et al., 1994; Galadini & Messina, 1994; Ghisetti & Vezzani, 1997; Cavinato et al., 2002; Patruno & Scisciani, 2021). Seismic reflection data show a half-graben geometry of the basin, with thickening of the sedimentary infill towards the eastern basin-bounding main fault, where the thickness of the sediments reaches up to 1,000 m (Fig. 2; Cavinato et al., 2002; Cella et al., 2021). The Quaternary continental deposits unconformably overlie Late Miocene turbidites and Mesozoic to Mid-Miocene carbonate bedrock (Giraudi, 1988; 1998; Patruno & Scisciani, 2021). The Fucino Basin hosted the largest lake of Central Italy, which was drained twice throughout its history: the first time in Roman period, the second time in 1862-1875. Since then, the former lacustrine area remained dry, and currently it represents one of the largest plains in Italy, measuring 20 km in the E-W direction and 10 km in the N-S direction, mostly exploited for agriculture. However, the Fucino basin is exploited also for industrial activities, especially close to the town of Avezzano, which lies on the western side of the basin (Fig. 2).

In 1915, the Fucino basin was struck by the destructive M7 Avezzano earthquake, which caused the complete destruction of several towns and villages and about 30,000 casualties (Fig. 2). The earthquake produced several coseismic effects, including

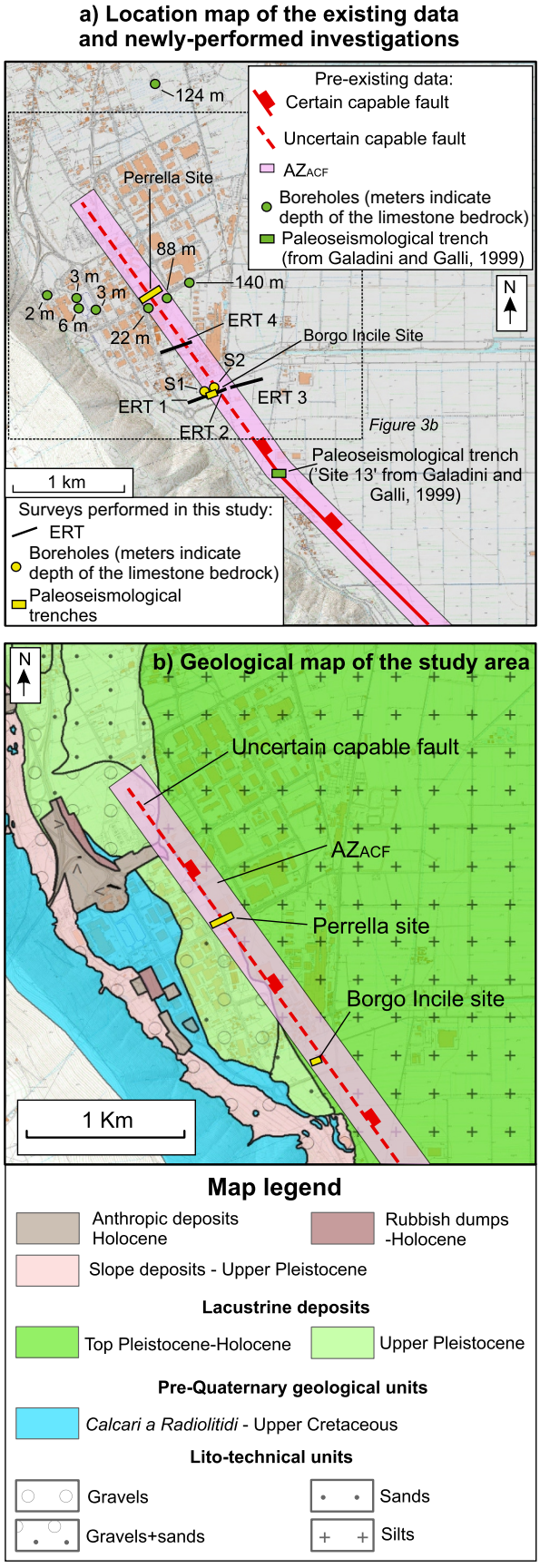

Fig. 3 - Investigations and geology in the surroundings of the Luco fault. a) Ensemble of the available and newly-performed investigations in the surroundings of the Luco fault. In green are pre-existing data, in yellow are the investigations performed within this study, in black are the ERT surveys performed during this study. b) Geological map of the Luco fault (modified after Di Naccio et al., 2020).

surface faulting in the form of a continuous scarp up to 1 m high and 23 km long along the San Benedetto-Gioia dei Marsi fault, as reported by eyewitnesses (Oddone, 1915; Serva et al., 1986; Michetti et al., 1996). Paleoseismological studies improved the knowledge of the distribution of surface ruptures associated with the 1915 earthquake, extending their along-strike length up to 38 km (Serva et al., 1986; Michetti et al. 1996; Galadini & Galli, 1999; Galli et al., 2012; Gori et al., 2017). Moreover, paleoseismological studies have shown that the 1915 earthquake has produced surface ruptures also on faults distributed parallel to the San Benedetto-Gioia dei Marsi fault, such as the Trasacco and the Luco faults (Fig. 2; Galadini & Galli, 1999). Overall, paleoseismology suggests that surface-rupturing earthquakes have repeatedly occurred through time in the Fucino Basin, with at least 10 seismic events observed since 32,520±500 years B.P., seven of which occurred during the Holocene, including a fault activation of the 5th-6th century AD and the already mentioned 1915 earthquake (Galadini & Galli, 1999). More recently, Galli et al. (2016) hypothesized the occurrence of another historical (Medieval) fault displacement, which is presently object of further paleoseismological investigations by one of the authors of the present paper (F. Galadini).

The Luco fault has been firstly identified by Giraudi (1986) in proximity of the village of Luco dei Marsi as an about 1 km-long lineament highlighted by the contact between soils with different lithologies and water content. Galadini & Galli (1999), through analysis of aerial photographs and paleoseismological investigations, extended the length of the Luco fault and provided first evidence of the occurrence of surface-rupturing earthquakes along the fault. Specifically, these authors have identified two surface-rupturing events in their "site 13" (Fig. 3a): (i) the 1915 earthquake and (ii) an earthquake subsequent to the Roman drainage of the lake (I-II century AD), for which the authors assign a time range between II and XV centuries AD and hypothesize it could be the earthquake of 484/508 AD, an event reported in the catalogues of historical seismicity and widely observed in paleoseismological trenches across the Fucino faults (e.g., Galadini & Galli, 1999). Both earthquakes caused a vertical offset of about 0.1-0.2 m. Effects of the earthquakes recorded on the Luco fault have also been recognised on other faults in the Fucino basin, suggesting therefore that the Luco fault ruptured together with them during those large earthquakes. Seismic reflection profiles crossed the surface trace of the Luco fault, but they were not able to visualize the fault at depth (Cavinato et al., 2002; Patruno et al., 2021).

In recent years, the seismic microzonation of Avezzano hypothesized the northward continuation of the Luco fault within the industrial district of the town. This is supported by the observation of the abrupt deepening of the interface between the lacustrine deposits and the limestone bedrock shown by two borehole data, occurring beneath the industrial area on a relatively-short map distance (deepening of 66 m over a map distance of 188 m; Perrella site in Fig. 3a; Di Naccio et al., 2020). This deepening has been originally interpreted as due to normal faulting, but more work is needed to unveil its nature.

METHODS

We carried out a set of indirect and direct investigations (ERT surveys, continuous-coring boreholes, paleoseismological trenches) in order to verify the possible northward prolongation of the Luco fault (Fig. 3). Although multiple investigation techniques can be applied for investigating capable faults (e.g., indirect investigations as seismic, electrical, magnetic, gravitational and radar imaging, direct investigations as trenching and stacked boreholes; Section 5, California Geological Survey, 2018), we think that the methods described herein are those that best apply to the site-specific geological context of our work area. That is because electrical resistivity measurements have the ability to produce rapid and accurate imaging of the geology beneath the surface in a context characterised by lithologies with high resistivity contrast such as lacustrine deposits and limestones, and paleoseismological trenching represents the most accurate approach to visualize a capable fault without surface expression.

Four Electrical Resistivity Tomography (ERT) surveys have been acquired in key sites, aimed at identifying evidence that can support the hypothesis of faulting within the uppermost sedimentary layers (Figs 3a and 4). The locations of the ERTs have been chosen in order to (i) investigate the AZ_{ACF} and its surroundings, so to include the possibility that the fault strike orientation may have varied moving northward from "Site 13", and therefore the actual fault trace may not coincide with the supposed trace of the seismic microzonation (ERT1, ERT2 and ERT3, Figs 3a and 4), and (ii) investigate suspected topographic scarps identified in the field (ERT4, Figs 3a and 4). For each ERT survey, we used 64 electrodes in combination with a IRIS Syscal-R2 resistivity meter; the spacing between electrodes ranged from 2 to 5 m, depending on the site. The raw data acquired in the field (apparent resistivity in Ωm) were inverted using the Res2DInv software (Loke and Barker, 1996) to produce resistivity sections. For each site, both the Wenner and the dipole-dipole electrode configurations have been used. Using the same length of the ERT survey, the former configuration is more suitable to investigate relatively larger depths, whereas the latter gives higher resolution in mapping lateral changes of resistivity. Because we obtained consistent results, for simplicity in the following we show the ERT results using only the Wenner configuration. The ERT1, ERT2 and ERT3 are located along a linear transect for a total length of about 660 m (Figs 3a and 4). ERT1 is 222 m long and it has been acquired with 2 m spacing between electrodes joining 3 roll-along multielectrode acquisition systems. ERT2 is 220.5 m long and it has been acquired with 3.5 m spacing between electrodes. ERT3 is 315 m long and it has been acquired with 5 m spacing between electrodes. ERT4 is 315 m long and it has been acquired with 5 m spacing between electrodes. The different lengths of the ERT surveys and spacing between electrodes are a function of the investigation depth that we wanted to image. That is because in general longer ERT surveys and larger spacing produce deeper imaging of the subsurface.

The lithological setting of the sites where we acquired the ERT surveys is characterized by alternating clays, sands and gravels deposited above the limestone bedrock (Giraudi, 1988; Giraudi, 1998; Cavinato et al., 2002; Di Naccio et al., 2020) (Fig. 3b). These

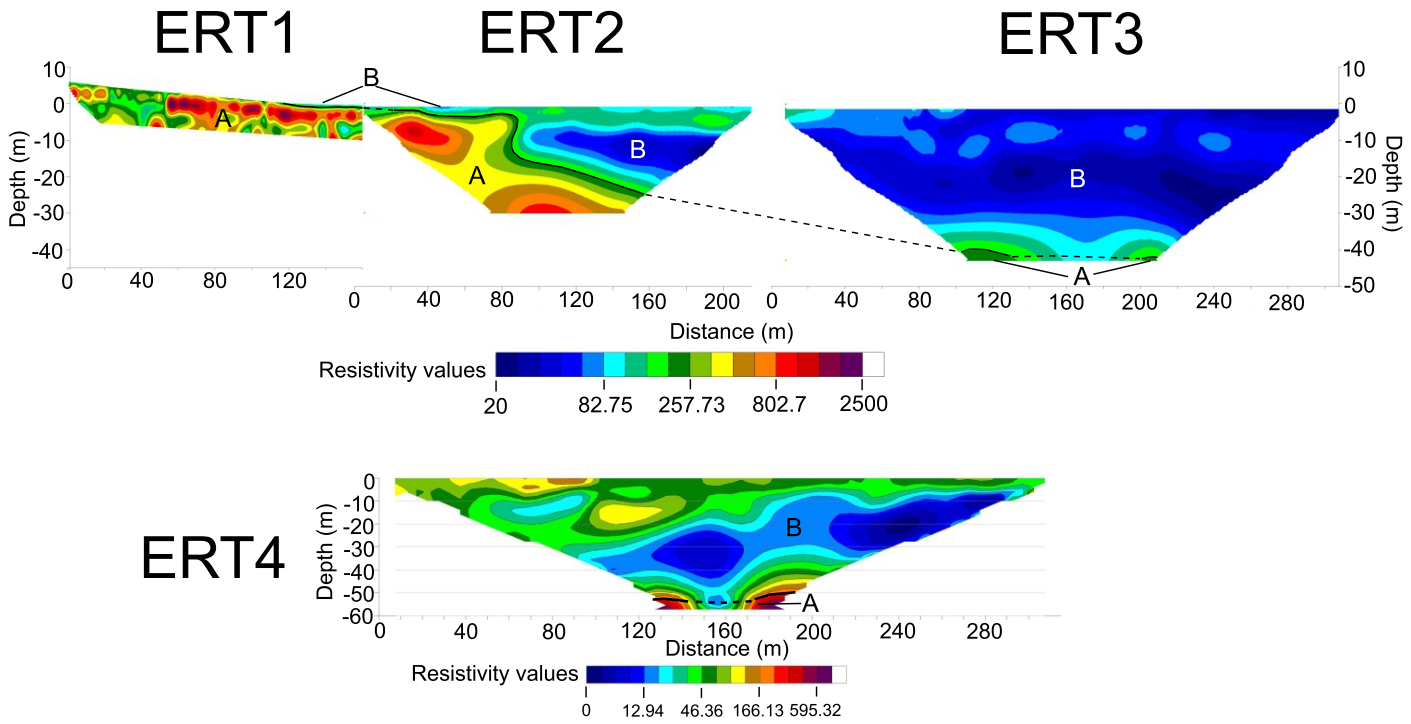

Fig. 4 - Newly-performed ERT investigations. We interpret bodies A as representative of carbonate bedrock, due to the high values of resistivity (generally above 300 Ωm). We interpret bodies B as representative of fluvio-lacustrine deposits. The black line represents the interface between the bodies A and B, dashed when supposed. The different depth reached by the ERT profiles are due to the different lengths and different spacing between the electrodes (longer the ERT survey, larger the spacing between electrodes, deeper the profile).

rocks have different resistivity values, thus the ERT surveys were able to provide a detailed reconstruction of the geological setting of the uppermost layers beneath the surface. Considering the local geology, we preliminary assume bodies with resistivity layers above 300 Ωm to belong to the limestone bedrock, whereas layers with lower values of resistivity to the fluvio-lacustrine deposits. Abrupt sub-vertical lateral variations in the resistivity values can be interpreted as faults juxtaposing layers with different resistivity (e.g., Cinti et al., 2015). However, the interpretation of such sub-vertical lateral changes of resistivity values as faults is not straightforward in complex morpho-sedimentary and tectonic settings like the Fucino basin, where these buried morphologies could be due to either tectonic or denudation-depositional processes. For instance, scarp-like morphologies shown by ERT profiles can be interpreted both as fault scarps or as paleocliffs associated with ancient lacustrine terraces. Moreover, results from geophysical investigations performed in urban areas can be biased by the presence of buried structures, such as pipelines, sewer, cavities, or by the water content of the subsurface. Therefore, direct investigations are required for interpreting these resistivity changes.

Where the ERT profiles have shown a sub-vertical discontinuity (the "Borgo Incile" site, Figs 3a, 5 and 6), we have performed two continuous-coring boreholes located 26 m to the west (S1) and 24 m to the east (S2) of the surface projection of the discontinuity. The two boreholes were planned in order to corroborate the stratigraphy reconstructed through the ERT surveys and to verify the depth of the limestone bedrock on both sides of the discontinuity. The depth of the boreholes is calibrated against the depth of the limestones. Furthermore, we have performed a paleoseismological trench to verify the nature of the sub-vertical discontinuity observed along the ERT profile. The trench was located within the two boreholes previously performed and along the trace of the ERT profile (Fig. 5). The trench is 44 m long and 2-3 m deep, and arranged with a benched layout, with one wall preserved vertical for investigation (Figs 6). We constrained chronological data by applying the Optically Stimulated Luminescence (OSL) dating methodology, due to the predominance of sand deposits in the stratigraphic record. Luminescence dating is used to date the time since grains of quartz or feldspar have been last exposed to sunlight or heat; it therefore calculates the timing of sand deposition and subsequent burial (Lian & Roberts, 2006). The dated sample has been collected within a well-preserved sandy unit, located in the lower (i.e., older) part of the trench wall. The luminescence dating has been performed by the PH3RDA laboratory at the University of Catania (Italy).

An additional paleoseismological survey was performed within the industrial district of Avezzano, to verify whether an active fault is responsible of the abrupt deepening of the bedrock as shown by the two boreholes ("the Perrella site"; see previous Section, Figs 3a and 7). The trench survey was organised in 4 different trenches, arranged in order to explore most of the AZ_{ACF} and to cross the hypothetical fault trace proposed by the seismic microzonation (Fig. 3a and 7a). This specific arrangement was necessary in order to avoid roads and power lines. Trench 1 is 83 m long, trench 2 is 8 m long, trench 3 is 23 m long and trench 4 is 27 m long. The trenches reach depths of 2.5-3 m. Chronological data have been collected with different approaches. We performed radiocarbon dating of two paleosols by measuring the concentration of ^{14}C within their organic material (calibration scheme adopted INTCAL13, see Bronk &

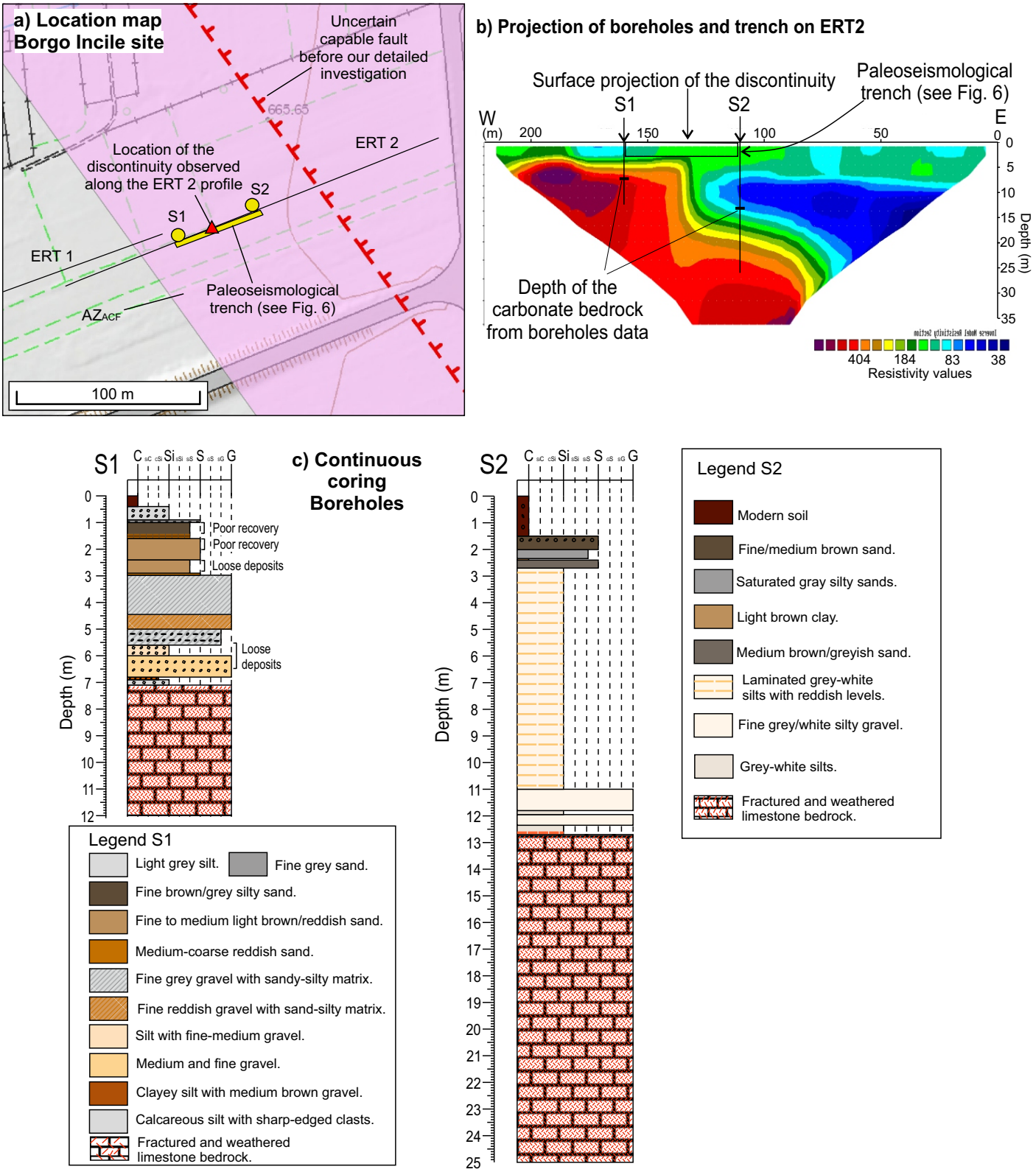

Fig. 5 - Exploring the Borgo Incile site. a) Location map of the investigations performed during this study together with the uncertain fault trace provided by the local seismic microzonation and its Attention zone. Black lines highlight the traces of the ERT surveys, yellow dots locate the boreholes, yellow rectangle indicate the paleoseismological trench, red triangle is the projection at surface of the discontinuity observed along the ERT2 profile. b) Projection of the boreholes and of the paleoseismological trench on the ERT2 profile. c) Stratigraphy of the boreholes S1 and S2.

Ramsey, 2009; Reimer et al., 2013; analysis performed at the Beta Analytic laboratory (Florida, USA). We have also obtained relative ages through archaeological observations of pottery material found within recent colluvial units and a basic tephrocronological analysis consisting in the mineralogical and lithological characterization of volcanoclastic deposits embedded in the stratigraphic record, by comparison with well-known volcanoclastic deposits found in the Fucino basin (e.g., Giaccio et al., 2017).

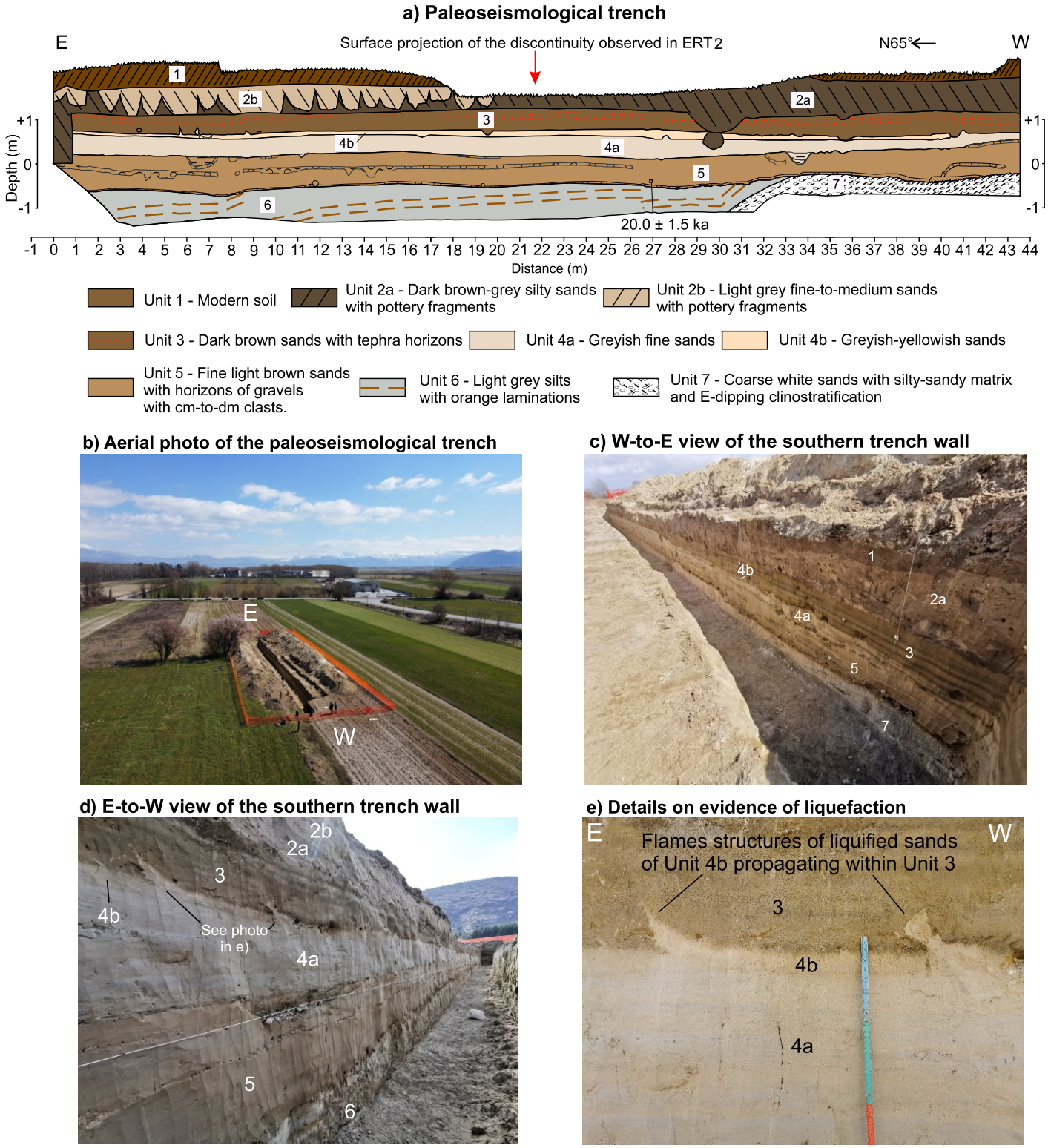

Fig. 6 - Paleoseismological trench in the Borgo Incile site. a) Stratigraphic log of the paleoseismological trench. b) Aerial photograph of the paleoseismological trench. c), d) Photographs of the trench walls, with reported the number of the stratigraphic units. e) Details on flame structures due to the liquefaction of sands in Unit 4b intruding within Unit 3.

RESULTS

Here we present the results of our investigations. Firstly, we present the results of the ERT surveys, and subsequently the results of the continuous-coring boreholes and of the paleoseismological surveys.

ERT surveys

The ERT1, ERT2 and ERT3 profiles show a body with high resistivity values, most likely to be the carbonate bedrock, that gently deepens towards east (body A in Fig. 4). However, the ERT2 profile shows an abrupt sub-vertical lateral variation in resistivity

values, at about 80 m distance along the profile (Fig. 4). Over this discontinuity, the top of the body A abruptly deepens by about 13 m, and this causes the juxtaposition of the high resistivity body A with bodies with low-to-medium resistivity values (body B). Moving eastward, the top of the body A continues to gently deepen towards the east, underneath continuous layers of rocks with low resistivity values, as shown by ERT3 (Fig. 4). Discontinuities showing geometries similar to the one of ERT2 have been commonly associated with buried fault scarps (e.g., Cinti et al., 2015). Moreover, the discontinuity is very close (about 60 m) to the supposed trace of the northern continuation of the Luco fault mapped during the seismic microzonation (Fig. 5a). Hence, we performed direct investigations along the trace of the ERT2 to verify the presence of a fault in this site (hereinafter called the Borgo Incile site), as shown in paragraph 4.2.

The ERT4 profile shows a mostly undisturbed stratigraphy, with layers with low-to-medium resistivity values distributed continuously along the profile. High resistivity values (A body) are located at a depth of about 50 m, without any evidence of lateral discontinuities that might suggest faulting. Overall, the ERT4 suggests the absence of faulting at this site.

The Borgo Incile site

Continuous coring boreholes

The S1 borehole is located 26 m west of the discontinuity, and it reaches a depth of 12 m (Figs 5b and 5c). The stratigraphy consists of sandy silts and silty sands for the first 3 m depth, and coarser sediments between 3 and 7.10 m depth. Below 7.10 m, the stratigraphy shows heavily weathered and fractured limestones belonging to the Late Cretaceous *Calcari a Radiolitidi* formation, in agreement with outcropping limestones along the nearby slope (Fig. 3a). As shown in Fig. 5b, the stratigraphy observed in S1 confirms that the high resistivity body to the west of the discontinuity is representative of weathered limestone bedrock, with resistivity values of about 300-400 Ωm.

The S2 borehole is located 24 m east of the discontinuity, and it reaches a depth of 25 m (Figs 5b and 5c). The stratigraphy consists of sands for the first 2.6 m, and a continuous stack of laminated silts down to 12.7 m, with coarser layers observed at 11 m and 12 m. Below 12.7 m, the stratigraphy is characterized by heavily fractured and weathered limestones of the *Calcari a Radiolitidi* formation.

Overall, the two boreholes present different stratigraphic successions on the two sides of the discontinuity, in good agreement with the ERT profile. The boreholes show that the top of the limestone bedrock is deeper in S2 than S1, in agreement with what shown by the ERT profile, although the difference in depth measured across the boreholes is smaller than the scarp height suggested by the ERT2 profile (5.6 m from the boreholes, 13 m from the ERT profile; Figs 5b and 5c).

Paleoseismological investigation

We performed a paleoseismological trench along the ERT2 profile and in between the two boreholes S1 and S2 (Fig. 5a). The excavated walls exposed prevalently fluvial and lacustrine sediments, which we have subdivided into seven different units (Fig. 6). Beneath Unit 1 (modern soil) lies Unit 2, characterised by dark silty sands (Sub-Unit 2a) and light grey fine-to-medium sands (Sub-Unit 2b) of colluvial origin and presence of pottery fragments. Underneath Unit 2, we identified three different sub-horizontal units of fine-grained greyish-brownish sands (Units 3, 4 and 5 of lacustrine origin). Unit 3 is characterised by dark brown sands and the presence of multiple tephra layers. Unit 4 is made mostly of greyish fine sands (Sub-Unit 4a), which turns into greyish-yellowish sands in the upper part of the unit (Sub-Unit 4b). Unit 5 is made of light brown fine sands, with interbedded thin layers and lens of gravels with centimetric-to-decimetric clasts. Unit 5 lies unconformably over the deeper layers (Units 6 and 7). Unit 6 is characterised by light-grey silts with orange laminations that are mostly planar along the trench wall and turns into a gentle E-dipping clinostratification in the western part of the trench, towards the contact between Unit 6 and the underlying Unit 7. The latter is characterised by coarse white sands with E-dipping clinostratification, possibly related to the deposition of gravel bars in a fluvio-lacustrine environment. The consistency of the clinostratification observed in Unit 6 and Unit 7 suggests that the two units are in stratigraphic contact.

Evidence of paleoliquefaction has been observed at the contact between Unit 3 and Unit 4, where dm-scale flame structures of sands belonging to Unit 4b intrudes within sands of the Unit 3 (Fig. 6e).

Overall, the continuity of the layers and of the erosional surface at the base of Unit 5 is preserved over the entire length of the excavated walls. There is no evidence of faulting or fractures in correspondence of the discontinuity shown by ERT2 survey and along the entire length of the trench (Fig. 6).

Chronology of the stratigraphic record

In order to constrain the age of the stratigraphic record shown by the paleoseismological trench, we applied the OSL dating methodology on a sample of sands collected from Unit 5 (Fig. 6), which provided a sample age of 20.0 ± 1.5 ka.

Perrella site

Paleoseismological investigations

The excavated walls of the four trenches exhibit a stratigraphic record made of colluvial (upper part of the exposed succession) and alluvial (lower part) sediments interbedded with pedogenetic horizons, which we have subdivided into 14 Units (Fig. 7c and 8). The Unit numbers were attributed according to their stratigraphic position in respect to the entire paleoseismological survey. Moving from west to east, Trenches 3 and 4 show that beneath the modern soil (Unit 1), yellow sands with planar lamination (Unit 3, possibly related to a shoreline environment) and cross-laminated fine-to-medium gravels with sandy matrix (Unit 4, related to alluvial deposition) are deposited over an erosional surface that cuts through a dense set of thin layers made by alternating: brown paleosols (Units 6, 8 and 10), fine calcareous white silt and sands (Units 5, 7, possibly a product of alluvial processes) and a layer of fine reddish sands (Unit 9, related

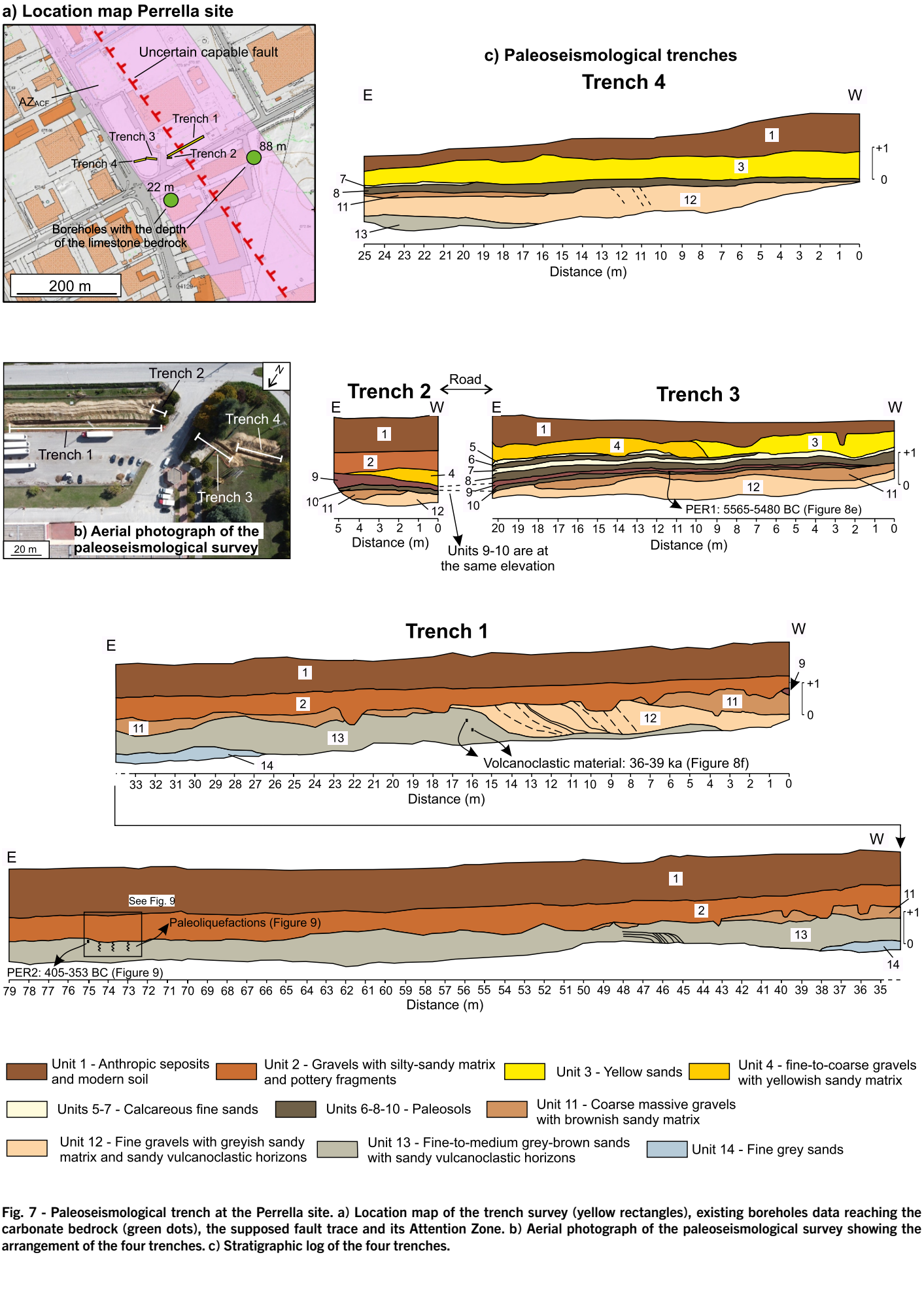

Fig. 7 - Paleoseismological trench at the Perrella site. a) Location map of the trench survey (yellow rectangles), existing boreholes data reaching the carbonate bedrock (green dots), the supposed fault trace and its Attention Zone. b) Aerial photograph of the paleoseismological survey showing the arrangement of the four trenches. c) Stratigraphic log of the four trenches.

to alluvial deposition). This succession lies unconformably over massive, channelized deposits of medium-to-coarse gravels (Unit 11, related to alluvial deposition) and cross-laminated yellowish-greyish gravels with sandy matrix (Unit 12, possibly related to a fluvio-lacustrine environment). In Trench 2, beneath the modern soil there is a brown eluvial-colluvial deposit, with calcareous clasts and pottery fragments (Unit 2) lying on an erosional surface that likely eroded almost the entire Unit 4. The set of paleosols and calcareous sands is no longer visible in Trench 2, except for Units 9 and 10. Unit 9 is in Trench 3 at the same elevation found in Trench 2, suggesting therefore that no faulting occurs in between the two trenches (i.e., under the road across which it was not possible to excavate). Unit 9 is visible also in the western termination of Trench 1, and it is located at the same elevation of Trench 2, allowing us to correlate the stratigraphic logs of the two trenches. Trench 1 shows a more regular stratigraphy, in which, beneath Units 1 and 2, channelized deposits of Unit 11 overlie an erosional surface cutting through cross-laminated fine gravels (Unit 12) and grey-brown fine-to-medium sands with clinostratification, with intercalation of black sands and gravels with dark sandy matrix (Unit 13, possibly related to fluvio-lacustrine environment). The dark matrix is characterised by a large content of volcanoclastic material (Fig. 8f). Towards the eastern termination of Trench 1, Unit 13 presents a pedogenic layer on its top, which formed at the expense of grey-brown sands. Unit 13 lies above fine, horizontally-laminated, grey sands (Unit 14).

Evidence of paleoliquefaction has been observed in the eastern termination of Trench 1, at distance 73-75 m (Fig. 9). Convolutions and flame structures of liquefied sands belonging to Unit 13 disrupt the pre-existing lamination. This liquefaction event caused the occurrence of localized depressions (craters) due to the sinking of the soil located in the uppermost part of Unit 13 (green pins marking the top of Unit 13 in Fig. 9).

Overall, there is no evidence of faulting along the entire extent of the paleoseismological survey performed at the Perrella site (Fig. 7c).

Chronology of the stratigraphic record

As mentioned in the Methods section, we constrained ages of the stratigraphic record through ^{14}C dating of two paleosols (PER1 and PER2, Fig. 7c) and a basic tephrochronological analysis (Figs 7c, 8e, 8f and 9). Sample PER1 has been collected from Unit 10 in trench 3 (Figs 7c and 8e). The age provided by the analysis is 5,565-5,480 BC. During the analysis, fragments of vegetal material have been found within the paleosol, which have been removed prior to the analysis. However, we cannot rule out the possibility that young carbon might have contaminated the sample we took from a sub-surficial horizon (i.e., the system was not closed). This could result in an underestimated ^{14}C age, younger than the actual age of the paleosol itself. The sample PER2 has been collected from the paleosol located at the top of Unit 13, towards the eastern termination of trench 1. Dating of PER2 constrains the *terminus post quem* of the liquefaction event described in paragraph 4.3.1. The age provided by the analysis is 405-353 BC.

We have performed mineralogical analyses of two samples of volcanoclastic material collected from the thin blackish layers embedded within Unit 13 (Fig. 8f). The volcanoclastic material is mostly characterised by blackish leucite- and clinopiroxene-bearing scoria clasts with abundant loose crystals of black and green clinopyroxene, leucite and large dark mica. The crystals

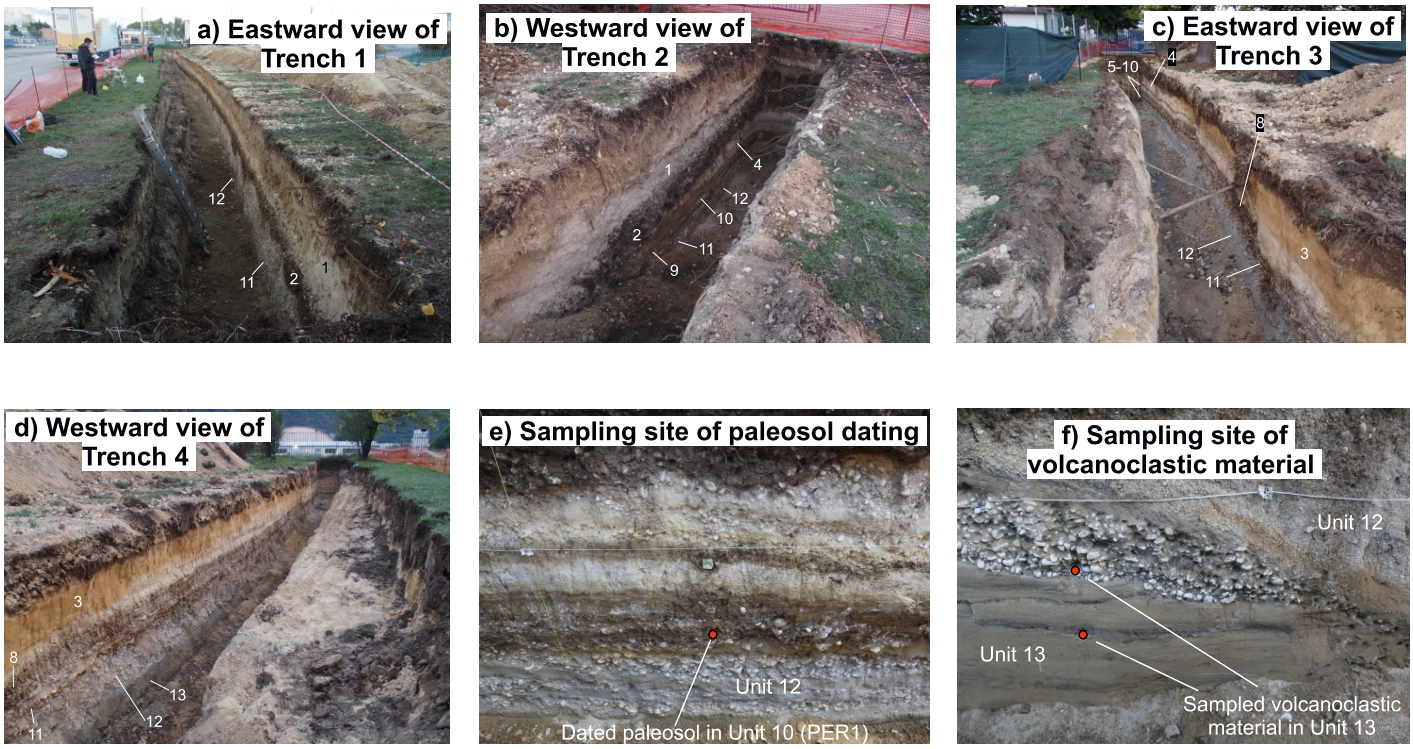

Fig. 8 - Photographs of the paleoseismological survey at the Perrella site. a), b), c) and d) Views of each of the four trenches. e) Paleosol sampled in Unit 10 (PER1). f) Sampled volcanoclastic material in Unit 13.

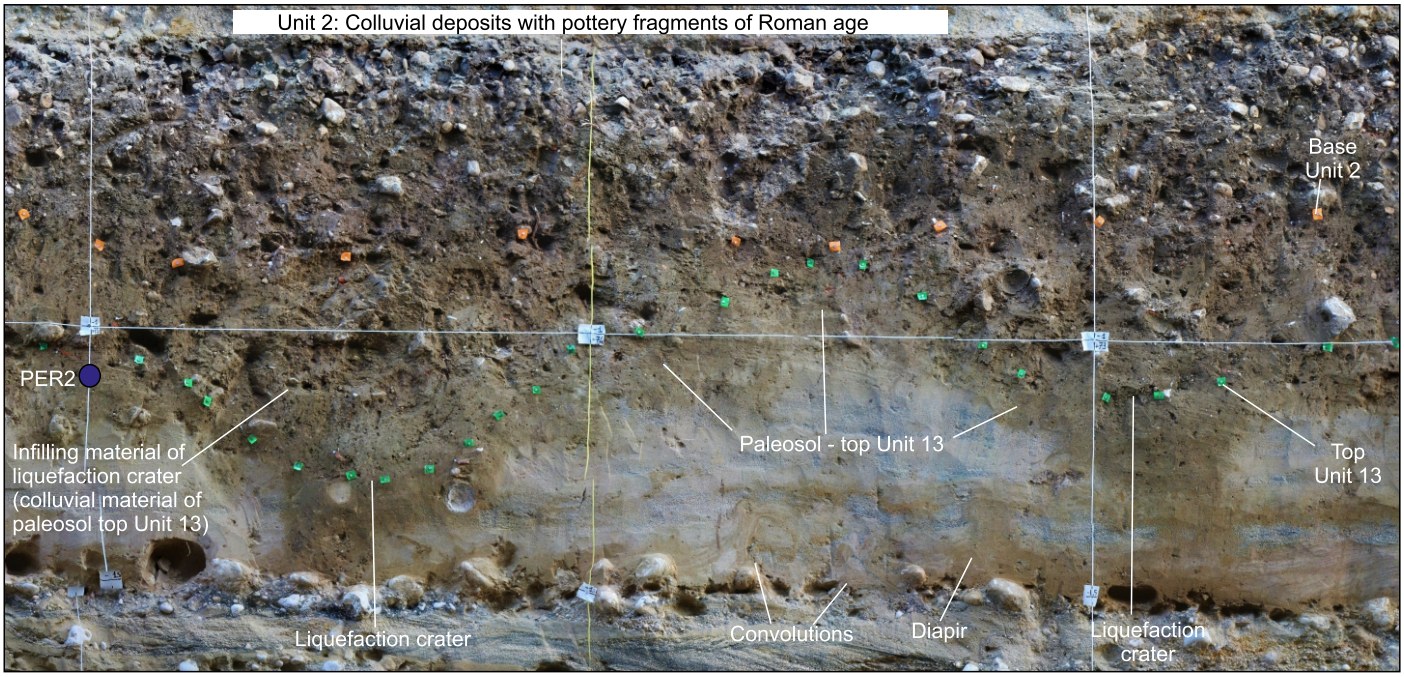

Fig. 9 - Liquefaction event at the Perrella site, 73-75 m distance along trench 1. Green pins mark the top of Unit 13; orange pins mark the base of the colluvial deposits of Unit 2. In the figure are highlighted convolutions, diapir-like structures and craters, all features that indicate the occurrence of liquefaction of sands within Unit 13. This caused the sinking of the pedogenic layer located at the top of Unit 13, creating craters subsequently infilled by the colluvial material derived by the same soil of Unit 13. Colluvial material of Unit 2 has subsequently sealed the liquefaction craters.

and their fragments are well preserved, with angular edges. Such lithological features and the general stratigraphic setting are typical and diagnostic of the products of the two most recent and intense eruptions of the Colli Albani volcanic complex, dated between 39 ka and 36 ka before present (BP) (Units 5 and 7 of the Colli Albani stratigraphy; Freda et al., 2006; Giaccio et al., 2007; 2009). These units form two widespread and really distinctive regional tephra markers for the Late Pleistocene sedimentary successions in Central Apennines (Narcisi 1994; Giraudi & Frezzotti, 1997; Giraudi, 1998; Giraudi et al., 2011; Giaccio et al., 2007; 2013; 2017; Galli et al., 2015).

DISCUSSION

The application of our multidisciplinary approach allowed us to explore the possible northward prolongation of the Luco fault trace and its relative AZ_{ACF} for most of its width in the industrial district of Avezzano. Through geophysical surveys and boreholes, we reconstructed the structural setting of the first tens of meters beneath the surface, identifying potential locations of faults within the AZ_{ACF} (Fig. 5). Subsequently, the paleoseismological trenches have verified whether these potential faults actually coincide with capable faults. Specifically, both paleoseismological surveys performed along the Luco fault did not show evidence of Late Pleistocene-Holocene faulting in the uppermost 2-3 m of the sedimentary record.

In the Borgo Incile site, the OSL dating of sands belonging to Unit 5 provided an age of 20.0 ± 1.5 ka, which supports the hypothesis of lacustrine deposition during the lake high standing phase of the Last Glacial Maximum (LGM) documented by the available literature (e.g., Giraudi, 1989; 1998). Given this age and the absence of structural discontinuities in the paleoseismological trench (Fig. 6), we infer that the Borgo Incile site did not experience surface faulting events at least for the last 20 kyrs and possibly for longer, given the lack of evidence of faulting also in the underlying and older Unit 6.

In the Perrella site, the potential contamination of PER1 suggests that we may have obtained an underestimated ^{14}C age, younger than the actual age of the paleosol. Therefore, we suggest that the paleosol in Unit 10 can be actually older than 5,565-5,480 BC. Sample PER2 dates the recent paleosol developed on the uppermost part of Unit 13, after the recent regression of the lake level (e.g., Giraudi et al., 1989) and the subaerial exposition of Unit 13; it therefore cannot be used to constrain the deposition age of Unit 13. The volcanoclastic sediments found in Unit 13 are dated 36-39 ka, as described in Section 4.3.2. However, although the volcanoclastic material found in Unit 13 is abundant and well-preserved, the nature of the deposits of Unit 13 does not allow us to exclude that such volcanoclastic material could have been reworked during the different stages of the lake evolution. Therefore, we cannot exclude that the sediments of Unit 13 could actually be younger than the volcanoclastic material found within it.

Overall, both paleoseismological surveys do not reach layers dated 40 ka, and therefore in theory we lack sufficient elements to exclude the presence of an active and capable fault in both the Borgo Incile and Perrella sites according to the definition of the Technical Commission on Seismic Microzonation (2015). However, we can make some further considerations on potential faulting events in both the Borgo Incile and Perrella sites by comparing the

results of our trenches with the data shown in Site 13 of Galadini & Galli (1999). As mentioned in Section 2, the authors identified paleoseismological evidence of two earthquakes occurred in 1915 and in Roman times (II-XV century AD, possibly the 484/508 AD event), with a minimum measurable offset of about 0.1-0.2 m for both earthquakes. Site 13 is located about 930 m and 2 km south of the Borgo Incile and the Perrella sites, respectively. Given the close distance between the three sites, we would have expected to find paleoseismological evidence of the two earthquakes also in both the Borgo Incile and Perrella sites, under the assumption that the Luco fault would propagate across them. Given the lack of evidence of these two historical earthquakes, we suggest that there are no capable faults in both the Borgo Incile and the Perrella sites. This leads us to multiple possible interpretations of the buried bedrock scarp shown by the ERT2 profile. One possible interpretation could be that the buried scarp is representative of an active non-capable fault. We do not have enough seismological data supporting this interpretation (for instance, the distribution of microseismicity data along the Luco fault), but we can make some considerations thanks to the available material. Firstly, the boreholes show that the limestone bedrock is characterised by the same formation on both sides of the scarp (*Calcari a Ratiolitidi* formation, Fig. 5). This suggests that whether the fault exists, its geological offset should be very small. Moreover, the borehole data show that the deepening of the limestone bedrock is actually less intense than what is suggested by the ERT (see Fig. 5). Hence, it may be possible that the scarp is less abrupt, and that a gentler deepening of the top of the limestone bedrock could explain the scarp shown in the ERT profile. Given these reasons, we prefer to interpret the scarp as a buried lacustrine paleocliff produced by the ancient lake level oscillations, with a shallower dip angle than what is hypothesized by the ERT profile. Features like this have been extensively observed along the flanks of the Fucino Basin (e.g., Giraudi, 1998). To explain the abrupt deepening shown by the limestone bedrock in the Perrella site, we believe that this could be representative of a steep deepening of the lake bed moving from a wave-cut platform located to the west of the Perrella site (as shown by multiple boreholes reaching the bedrock at 2-6 m in Fig. 3a) towards the centre of the basin, to the east of the site. This trend is supported by another borehole located ca. 250 m east of the Perrella site that reaches the bedrock at 140 m depth (Fig. 3a).

Overall, our interpretation suggests that the Luco fault does not propagate northwards and beneath the industrial district of Avezzano, but it probably tips out between site 13 of Galadini & Galli (1999) and our Borgo Incile site (Fig. 10). Specifically, we suggest that the fault tip could be located where, moving northwards from the Site 13, the slope loses its rectilinear geometry (Fig. 10). This new perspective for the industrial district of Avezzano has significant bearing upon the mitigation of the FDH. In fact, the industrial district of Avezzano should be removed from the AZ_{ACF} of the Luco fault, allowing therefore the construction of new buildings and other man-made infrastructures in the area (Fig. 10).

On the other hand, both paleoseismic investigations have shown evidence of earthquake-induced paleoliquefactions in the form of flame structures in the Borgo Incile site (Fig. 6) and an ensemble of convolutions, craters and diapir-like structures in the Perrella site (Fig. 9). These observations, combined with other studies in the region (Galli, 2000; Boncio et al., 2018; 2020), demonstrates the widespread occurrence and severity of this phenomenon in a lacustrine environment such as the Fucino basin. In addition to this, the dating of the sedimentary units in the Perrella site helps us to speculate about which earthquake may be responsible for the occurrence of paleoliquefaction. The liquefaction event caused the sinking of the soil located in the uppermost part of Unit 13, which dated 405-353 BC (Fig. 9). This soil should have therefore been exposed at the surface when the liquefaction event occurred. Hence, we can interpret the paleosol at the top of Unit 13 as the event-horizon of the earthquake causing this liquefaction event, representing therefore the *terminus post quem* of the earthquake responsible for such liquefaction. Subsequently, the liquefaction craters have been filled up by colluvial material derived by the reworked soil of Unit 13 (Fig. 9). Finally, the deposition of the clast-enriched colluvial deposits of Unit 2 (orange pins marking its base in Fig. 9) sealed the craters and their infilling. In fact, the base of Unit 2 is not affected by the sinking of the liquefaction craters, and therefore we can infer that Unit 2 has been deposited after the craters have been filled up. Hence, Unit 2 represents the *terminus ante quem* of the earthquake. Considering the obtained ^{14}C age and the presence of pottery fragments of roman age within Unit 2, we suggest that the earthquake responsible for liquefactions observed at the Perrella site could be that of 484/508 AD, an event widely recognised in the Fucino basin (see Galadini & Galli, 1999, for details). If this interpretation is correct, the 484/508 AD earthquake would have produced liquefaction in the site but not surface faulting.

As mentioned in the Introduction, there is a scarcity of studies describing approaches for investigating capable faults and for the mitigation of the FDH in urban areas following the publication of the Italian guidelines. We believe that the approach herein proposed could represent a pilot example for practical applications of the guidelines in Italy but also in other similar seismotectonic contexts elsewhere. This is because the Italian territory has plenty of towns and critical facilities potentially affected by capable faults, and, in this perspective, our paper may contribute to consolidate standard procedures and approaches for their investigation. Our study reiterates the importance of performing multidisciplinary approaches to disentangle data of equivocal genesis and nature (e.g., buried vertical contacts and scarps). In particular, the combined use of geophysical and paleoseismological surveys proves itself as a powerful and key approach for addressing the FDH issue. Specifically, our results show that only direct investigations, such as paleoseismological surveys, provide conclusive responses when the presence of capable faults is uncertain. In fact, although subsurface imaging techniques are easier and less demanding than paleoseismological investigations in terms of time, logistics and costs, the results they provide could lead to misleading interpretations, especially in regions characterised by a complex geological history. Therefore, we suggest that indirect geophysical investigations, such as ERT surveys, should always be supported by paleoseismological trenching.

The Italian guidelines for the management for capable faults consider 40 ka as the time limit for considering a fault as

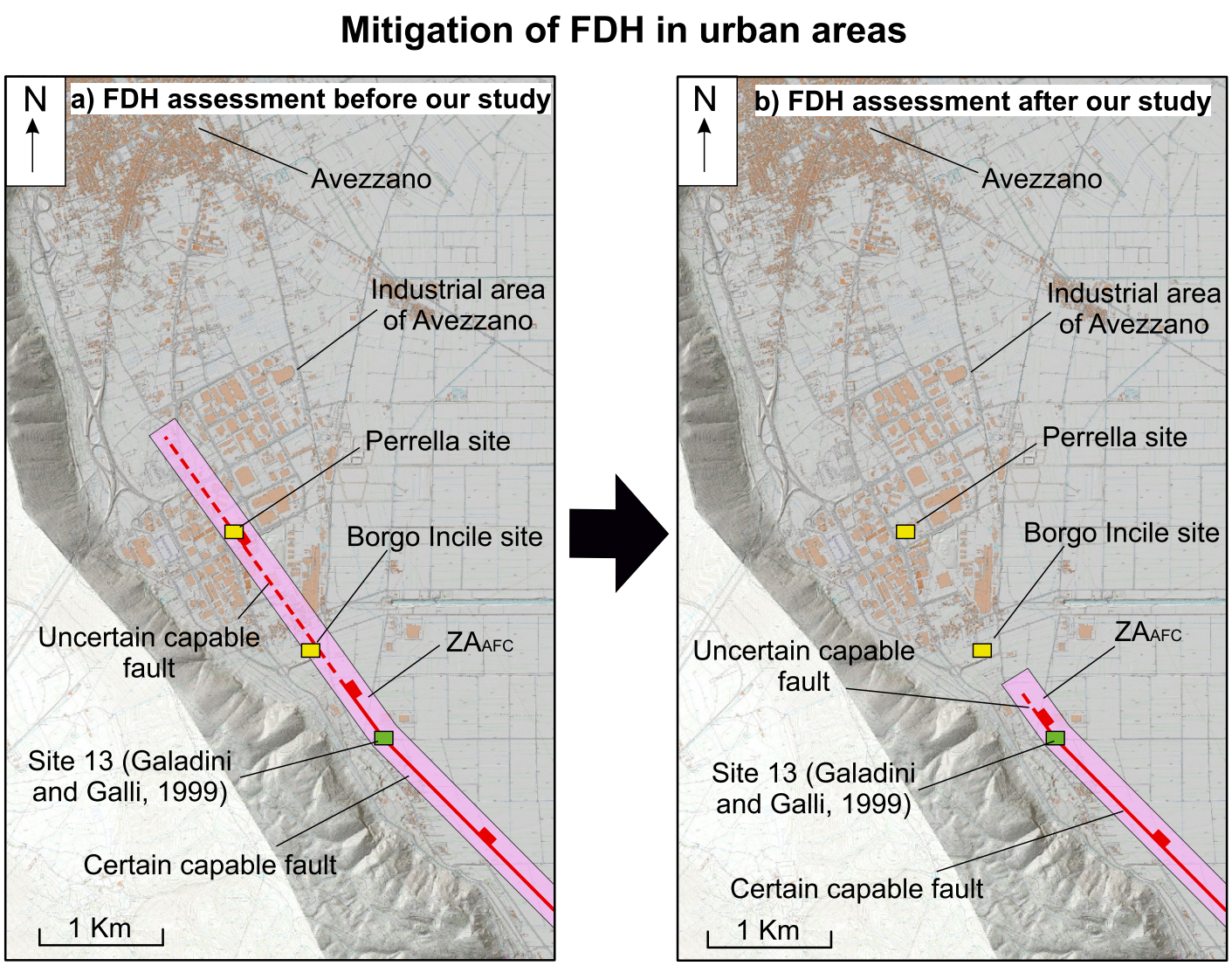

Fig. 10 - Mitigation of the Fault Displacement Hazard (FDH). a) FDH assessment prior to our study, with an uncertain fault trace running across the industrial district of Avezzano and an Attention zone built around the fault trace. b) FDH assessment after our study, with the newly-proposed fault trace of the Luco fault.

active (Technical Commission on Seismic Microzonation, 2015). However, our study shows that, in geological domains with high sedimentation rates and long earthquake recurrence intervals, standard paleoseismological surveys might not be deep enough to allow studying rock succession 40 ka old. In such cases, very deep trenching is needed, as documented in several studies worldwide (e.g., Audemard, 2005; McCalpin, 2009). However, trenches of greater depth are difficult to be executed in urban areas, as they require large spaces to be performed, and in some cases they may not even be possible. In these situations, other approaches should be applied in order to verify the presence of capable faults, according to the site-specific characteristics (e.g., Dolan et al., 2003).

Moreover, although the Italian guidelines suggest that faults sealed off by deposits older than 40 kyrs are likely to be considered inactive or, in any case, indicative of a low risk (unless they interfere with facilities of intrinsic high risk), the same guidelines do not suggest specific recommendations on how to demonstrate fault inactivity or non-capability. On the other hand, there are several geologic conditions where the inactivity or non-capability of a fault is very difficult or impossible to be demonstrated. These are the cases, for example, of faults without datable recent materials (e.g., bedrock faults), or faults with low slip rates in contexts of high sedimentation rate. We suggest that, taking in mind the impact that the decision will have on the territory, the conclusion about fault activity/inactivity or capability/non-capability should be made from the overall evaluation of the gathered constraints at the end of a multidisciplinary study, also of the regional seismotectonic setting. Therefore, we point out that the final decision should not be contingent upon only the ability of constraining the relations with sediments older or younger than 40 kyrs. In the present case study, the available data suggest us the non-capability of the fault. Even if we assume a blind fault, potentially capable of rupturing the ground surface in an unconstrained time span, we should consider a return period for such an unpredictable event of >20 kyrs. Possibly, such a level of FDH in active areas like the Fucino basin is difficult, if not impossible, to be spatially constrained in a way of practical application (i.e., fault zoning) and it therefore falls within the epistemic uncertainties.

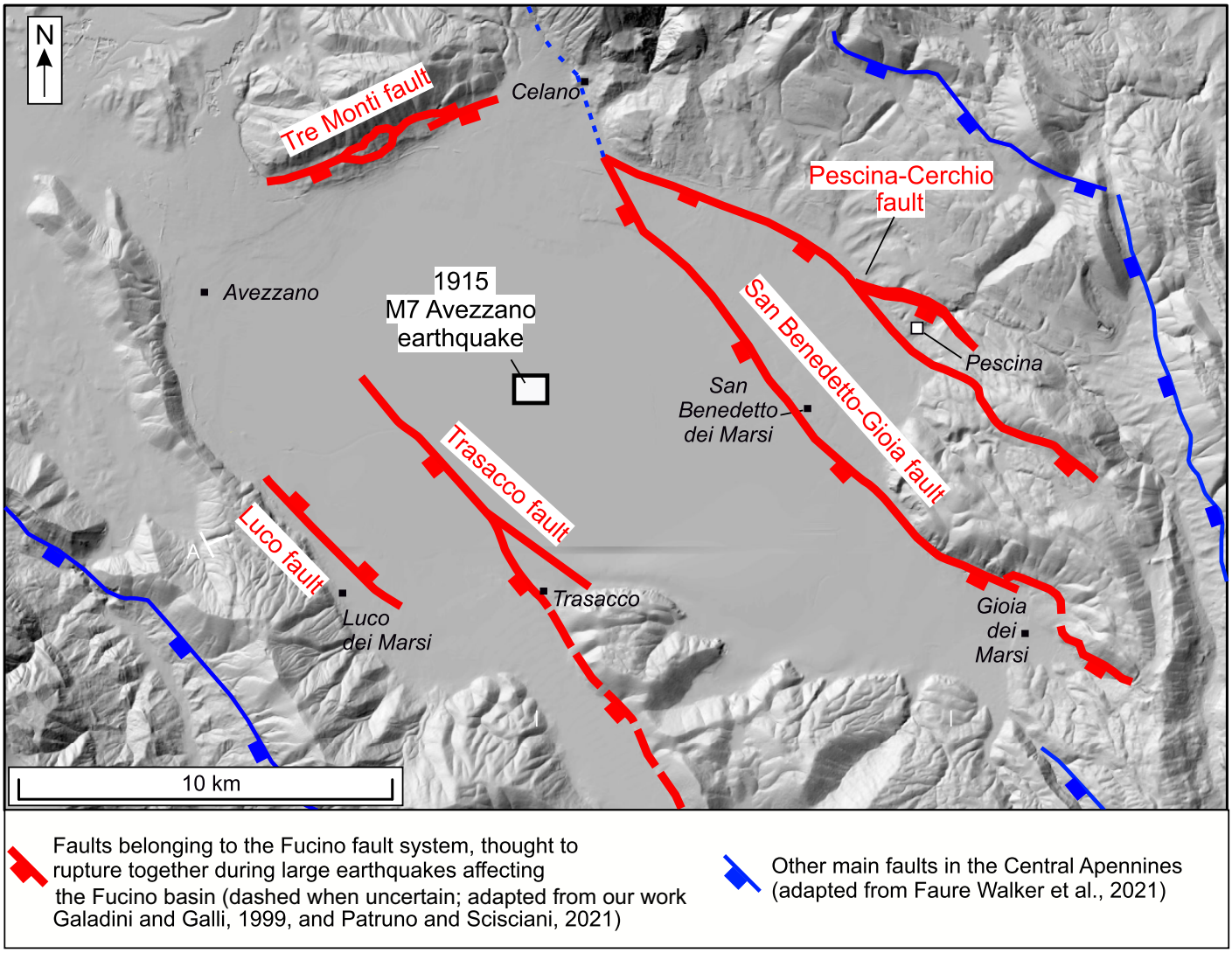

Fig. 11 - New fault map for the Fucino basin, with the new trace of the Luco fault as defined in this work. Red traces are the principal active faults of the Fucino basin, thought to be able to rupture simultaneously during large earthquakes (modified after our work, Galadini and Galli, 1999, and Patruno and Scisciani, 2021). In blue are other main faults of the Central Apennines (adapted from Faure Walker et al., 2021).

From a geological point of view, the trace of the Luco fault is likely confined within the trace of the Trasacco fault (Fig. 11). In our view, this finding suggests that the Luco fault could be an anthitetic fault of the Trasacco fault, and it ruptures only during strong earthquakes rupturing the Trasacco fault. Moreover, as shown by paleoseismological studies, the Trasacco-Luco faults pair could also rupture during large earthquakes occurring on the main W-dipping faults bordering the eastern flank of the Fucino basin (e.g., Galadini and Galli, 1999; Fig. 11). Our new findings provide useful information for databases of active faults in the Italian territory, which should be updated accordingly (e.g., the ITHACA database, ITHACA Working Group, 2019; the Fault2Sha database, Faure Walker et al., 2021).

CONCLUSIONS

We have presented a multidisciplinary approach that combines and integrates geophysical techniques and paleoseismological surveys to study capable faults in urbanised areas at different scales. This approach allowed us to demonstrate, with reasonable certainty, the absence of the northward prolongation of the Luco fault within the industrial district of Avezzano. Our study shows that uncertain fault traces can be solved by applying subsurface imaging, continuous coring boreholes and paleoseismological trenches. This provides key information for mitigating the FDH in urban areas hosting important infrastructures for the society. In general, the Italian Guidelines for FDH indicate paleoseismological trenches as the most significant survey for the investigation of capable faults. Our results support and consolidate this indication, suggesting that indirect subsurface imaging techniques, when applied in complex geological contexts and in urban areas, could provide information that may be open to multiple interpretations. Therefore, we recommend that geophysical surveys should always be supported by paleoseismic investigations in order to mitigate the FDH. Given the short time since the publication of the Italian Guidelines regarding FDH, we believe that the results of this study, which allowed us to reasonably exclude the hazard from surface

faulting in an industrial district, have methodological implications for other similar applications elsewhere in the Italian and other similar geological contexts.

ACKNOWLEDGEMENTS

This work was funded by Regione Abruzzo local authority (PORFESR, IV, 3.1.c) and Italian National Department of Civil Protection (DPC) (art. 11, DL 39/2009) within the agreements between Regione Abruzzo and "G. d'Annunzio" University of Chieti-Pescara, Departments DiSPuTer and INGEO (Resp. P. Boncio) and Istituto Nazionale di Geofisica e Vulcanologia, Rome and L'Aquila (Resp. G. Milana). Scientific papers funded by DPC do not represent its official opinion and policies. We thank the Azienda Regionale per le Attività Produttive (ARAP) of the Abruzzo Region and Dr. A. Perrella for their availability and financial support for excavating the trenches in the Perrella site. We thank Alessandro Maria Michetti for his useful comments to an early version of this manuscript. We thank the Associate Editor Giulio Viola, Marco Mercuri and Thomas Gusmeo for their useful comments that helped improving the manuscript.

REFERENCES

Audemard M.F.A. (2005) - Paleoseismology in Venezuela: Objectives, methods, applications, limitations and perspectives. Tectonophysics, 408(1-4), 29-61, https://doi.org/10.1016/j.tecto.2005.05.034.

Baize S., Nurminen F., Sarmiento A., Dawson T., Takao M., Scotti O., Azuma T., Boncio P., Champenois J., Cinti F.R. & Civico R. (2020) - A worldwide and unified database of surface ruptures (SURE) for fault displacement hazard analyses. Seismological Research Letters, 91(1), 499-520, https://doi.org/10.1785/0220190144.

Boncio P., Galli P., Naso G. & Pizzi A. (2012) - Zoning Surface Rupture Hazard along Normal Faults: Insight from the 2009 Mw 6.3 L'Aquila, Central Italy, Earthquake and Other Global Earthquakes, Bulletin of the Seismological Society of America, 102, 918-935, https://doi.org/10.1785/0120100301.

Boncio P., Amoroso S., Vessia G., Francescone M., Nardone M., Monaco P., Famiani D., Di Naccio D., Mercuri A., Manuel M.R. & Galadini F. (2018) - Evaluation of liquefaction potential in an intermountain Quaternary lacustrine basin (Fucino basin, central Italy). Bulletin of Earthquake Engineering, 16(1), 91-111, https://doi.org/10.1007/s10518-017-0201-z.

Boncio P., Amoroso S., Galadini F., Galderisi A., Iezzi G. & Liberi F. (2020) - Earthquake-induced liquefaction features in a late Quaternary fine-grained lacustrine succession (Fucino Lake, Italy): Implications for microzonation studies. Engineering Geology, 272, 105621.

Bronk Ramsey C. (2009) - Bayesian analysis of radiocarbon dates. Radiocarbon, 51(1), 337-360.

Bryant W.A. & Hart E.W. (2007) - Fault-Rupture Hazard Zones in California: Alquist-Priolo Earthquake Fault Zoning Act with Index to Earthquake Fault Zones Maps, California Geological Survey, Special Publication 42, 41 pp.

California Geological Survey, Special Publication 42 (2018, 12th revision) - Earthquake Fault Zones: A guide for government agencies, property owners/developers, and geoscience practitioners for assessing fault rupture hazards in California, https://www.conservation.ca.gov/cgs/Documents/Publications/Special-Publications/SP_042.pdf

Cavinato G.P., Carusi C., Dall'Asta M., Miccadei E. & Piacentini T. (2002) - Sedimentary and tectonic evolution of Plio–Pleistocene alluvial and lacustrine deposits of Fucino Basin (central Italy). Sedimentary Geology, 148(1-2), 29-59.

Cella F., Nappi R., Paoletti V. & Florio G. (2021) - Basement Mapping of the Fucino Basin in Central Italy by ITRESC Modeling of Gravity Data. Geosciences, 11(10), 398.

Cinti F.R., Pauselli C., Livio F., Ercoli M., Brunori C.A., Ferrario M.F., Volpe R., Civico R., Pantosti D., Pinzi S. & De Martini P.M. (2015) - Integrating multidisciplinary, multiscale geological and geophysical data to image the Castrovillari fault (Northern Calabria, Italy). Geophysical Supplements to the Monthly Notices of the Royal Astronomical Society, 203(3), 1847-1863 https://doi.org/10.1093/gji/ggv404.

Di Naccio D., Famiani D., Liberi F., Boncio P., Cara F., De Santis A., Di Giulio G., Galadini F., Milana G., Rosatelli G. & Vassallo M. (2020) - Site effects and widespread susceptibility to permanent coseismic deformation in the Avezzano town (Fucino basin, Central Italy): Constraints from detailed geological study. Engineering Geology, 270, 105583, https://doi.org/10.1016/j.enggeo.2020.105583.

Dolan J.F., Christofferson S.A. & Shaw J.H. (2003) - Recognition of paleoearthquakes on the Puente Hills blind thrust fault, California. Science, 300(5616), 115-118.

Faure Walker J., Boncio P., Pace B., Roberts G., Benedetti L., Scotti O., Visini F. & Peruzza L. (2021) - Fault2SHA Central Apennines database and structuring active fault data for seismic hazard assessment. Scientific data, 8(1), 1-20.

Ferrario M.F. & Livio F. (2021) - Conditional probability of distributed surface rupturing during normal-faulting earthquakes. Solid Earth, 12(5), 1197-1209.

Freda C., Gaeta M., Karner D.B., Marra F., Renne P.R., Taddeucci J., Scarlato P., Christensen J.N. & Dallai L. (2006) - Eruptive history and petrologic evolution of the Albano multiple maar (Alban Hills, Central Italy). Bulletin of Volcanology, 68(6), 567-591.

Galadini F. & Messina P. (1994) - Plio-Quaternary tectonics of the Fucino basin and surrounding areas (central Italy). Giornale di Geologia, 56(2), 73-99.

Galadini F. & Galli P. (1996) - Paleoseismology related to deformed archaeological remains in the Fucino Plain. Implications for subrecent seismicity in central Italy. Annali di Geofisica, 34(5), 925-940.

Galadini F. & Galli P. (1999) - The Holocene paleoearthquakes on the 1915 Avezzano earthquake faults (central Italy): implications for active tectonics in the central Apennines. Tectonophysics, 308(1-2), 143-170.

Galadini F. & Galli P. (1999) - Paleoseismology related to the displaced Roman archaeological remains at Egna (Adige valley, northern Italy). Tectonophysics, 308, 171-191

Galadini F., Galli P. & Giraudi C. (1997) - Paleosismologia della Piana del Fucino (Italia Centrale). Il Quaternario, 10 (1), 27-64.

Galadini F., Galli P. & Giraudi C. (1999) - Analisi paleo sismologiche nell'area della piana del Fucino. In: 13 gennaio 1915: Il terremoto nella Marsica, Castenetto & Galadini (eds.), SSN-CNR, Roma, pp. 223-242.

Galadini F., Ceccaroni E., Dixit Dominus G., Falcucci E., Gori S., Maceroni D., Bonasera M., Di Giulio G., Moro M., Saroli M. & Vassallo M. (2022) - Combining earth sciences with archaeology to investigate natural risks related to the cultural heritage of the Marsica region (central Apennines, Italy). Mediterranean Geoscience Reviews, 4(3), 287-318.

Galli P. (2000) - New empirical relationships between magnitude and distance for liquefaction. Tectonophysics, 324(3), 169-187.

Galli P. & Galadini F. (2003) - Disruptive earthquakes revealed by faulted archaeological relics in Samnium (Molise, southern Italy). Geophysical Research Letters, 30, 1266, 70/1-4.

Galli P. & Naso G. (2009) - Unmasking the 1349 earthquake source (southern Italy). Paleoseismological and archaeoseismological indications from the Aquae Iuliae fault. Journal of Structural Geology, 31, 128-149.

Galli P., Galadini F. & Calzoni F. (2005) - Surface faulting in Norcia (central Italy): a "paleoseismological perspective". Tectonophysics, 403, 117-130

Galli P., Peronace E. & Messina P. (2022) - Archaeoseismic Evidence of Surface Faulting in 1703 Norcia Earthquake (Central Italian Apennines, Mw 6.9). Geosciences, 12(1), 14, https://doi.org/10.3390/geosciences12010014.

Galli P., Giaccio B., Peronace E. & Messina P. (2015) - Holocene paleoearthquakes and early-late Pleistocene slip rate on the Sulmona Fault (Central Apeninnes, Italy). Bulletin of the Seismological Society of America, 105(1), 1-13.

Galli P., Giaccio B., Messina P. & Peronace E. (2016) - Three magnitude 7 earthquakes on a single fault in central Italy in 1400 years, evidenced by new palaeoseismic results. Terra Nova, 28(2), 146-154.

Galli P., Messina P., Giaccio B., Peronace E. & Quadrio B. (2012) - Early Pleistocene to late Holocene activity of the Magnola fault (Fucino fault system, central Italy). Boll. Geofis. Teor. Appl. 53, 435-458.

Giaccio B., Sposato A., Gaeta M., Marra F., Palladino D.M., Taddeucci J., Barbieri M., Messina P. & Rolfo M.F. (2007) - Mid-distal occurrences of the Albano Maar pyroclastic deposits and their relevance for reassessing the eruptive scenarios of the most recent activity at the Colli Albani Volcanic District, Central Italy. Quaternary International, 171-172, 160-178, https://doi.org/10.1016/j.quaint.2006.10.013.

Giaccio B., Marra F., Hajdas I., Karner D.B., Renne P.R. & Sposato A. (2009) - $^{40}Ar/^{39}Ar$ and ^{14}C geochronology of the Albano maar deposits: Implications for defining the age and eruptive style of the most recent explosive activity at Colli Albani Volcanic District, Central Italy. Journal of Volcanology and Geothermal Research, 185(3), 203-213, https://doi.org/10.1016/j.jvolgeores.2009.05.011.

Giaccio B., Arienzo I., Sottili G., Castorina F., Gaeta M., Nomade S., Galli P. & Messina P. (2013) - Isotopic (Sr–Nd) and major element fingerprinting of distal tephras: an application to the Middle-Late Pleistocene markers from the Colli Albani volcano, central Italy. Quaternary Science Reviews, 67, 190-206, https://doi.org/10.1016/j.quascirev.2013.01.028.

Giaccio B., Niespolo E.M., Pereira A., Nomade S., Renne P.R., Albert P.G., Arienzo I., Regattieri E., Wagner B., Zanchetta G. & Gaeta M. (2017) - First integrated tephrochronological record for the last~ 190 kyr from the Fucino Quaternary lacustrine succession, central Italy. Quaternary Science Reviews, 158, 211-234.

Giraudi C. (1986) - Faglie ad attività olocenica nella piana del Fucino (Abruzzo). Mem. Soc. Geol. It., 35, 875-880.

Giraudi C. (1988) - Evoluzione geologica della piana del Fucino (Abruzzo) negli ultimi 30.000 anni. Il Quaternario, 1(2), 131-159.

Giraudi C. (1989) - Lake levels and climate for the last 30,000 years in the Fucino area (Abruzzo-central Italy) a review. Palaeogeography, Palaeoclimatology, Palaeoecology, 70, 249-260.

Giraudi C. (1998) - Late Pleistocene and Holocene lake-level variations in Fucino Lake (Abruzzo, Central Italy) inferred from geological, archaeological and historical data. In: Harrison, S.P., Frezel, B., Huckriede, U., Weib, M.M. (Eds.), Paleaeohydrology as Reflected in Lake-level Changes as Climatic Evidence for Holocene Times, Gustav Fischer Verlag, Stuttgart, pp. 1-17.

Giraudi C. & Frezzotti M. (1997) - Late Pleistocene glacial events in the central Apennines, Italy. Quaternary Research 48, 280-290.

Ghisetti F. & Vezzani L. (1997) - Interfering paths of deformation and development of arcs in the fold-and-thrust belt of the central Apennines (Italy). Tectonics, 16(3), 523-536.

Gori S., Falcucci E., Galadini F., Moro M., Saroli M. & Ceccaroni E. (2017) - Geoarchaeology and paleoseismology blends to define the Fucino active fault slip history, Italy. Quaternary International, 451, 114-128.

IAEA (2015) - The Contribution of Palaeoseismology to Seismic Hazard Assessment in Site Evaluation for Nuclear Installations, IAEA TECDOC 1767). https://www-pub.iaea.org/MTCD/Publications/PDF/TE1767_web.pdf.

IAEA (2022) - Seismic Hazards in Site Evaluation for Nuclear Installations. Specific Safety Guide. IAEA Safety Standards. Series SSG-9 (Rev. 1) https://www.iaea.org/publications/14665/seismic-hazards-in-siteevaluation-for-nuclear-installations.

ITHACA Working Group (2019) - ITHACA (ITaly HAzard from CApable faulting), A database of active capable faults of the Italian territory. Version December 2019, ISPRA Geological Survey of Italy. Web Portal http://sgi2.isprambiente.it/ithacaweb/Mappatura.aspx.

Lavecchia G., Brozzetti F., Barchi M., Menichetti M. & Keller J.V. (1994) - Seismotectonic zoning in east-central Italy deduced from an analysis of the Neogene to present deformations and related stress fields, Geological Society of America Bulletin, 106(9), 1107-1120.

Lian O.B. & Roberts R.G. (2006) - Dating the Quaternary: progress in luminescence dating of sediments, Quaternary Science Reviews, 25, 2449-2468.

Loke M.H. & Barker R.D. (1996) - Rapid least-squares inversion of apparent resistivity pseudosections by a quasi-Newton method, Geophysical prospecting, 44(1), 131-152.

Maceroni D., Racano S., Falcucci E., Gori S. & Galadini F. (2018) - Application of Quaternary studies for the assessment of active and capable faults in the central Apennines: Implications for microzonation and seismotectonic analyses. Alpine and Mediterranean Quaternary, 31 (1), 221-224.

Maceroni D., Falcucci E., Gori S., Motti A., Moro M., Saroli M., Dominus G.D., Doumaz F. & Galadini F. (2022) - Assessing active and capable faulting as best practice for post-earthquake reconstruction activities: the Sant'Eutizio Abbey case study, in the epicentral area of the 2016 central Italy seismic sequence. Annals of Geophysics, 65(1).

McCalpin J.P. (2009) - A Field Techniques in Paleoseismology—Terrestrial Environments. International Geophysics, 95, 29-118.

Michetti A.M., Brunamonte F., Serva L. & Vittori E. (1996) - Trench investigations of the 1915 Fucino earthquake fault scarps (Abruzzo, Central Italy): geological evidence of large historical event, Journal of Geophysical Research: Solid Earth, 101(B3), 5921-5936.

Moss R.E.S. & Ross Z.E. (2011) - Probabilistic fault displacement hazard analysis for reverse faults. Bulletin of the Seismological Society of America, 101(4), 1542-1553.

Nurminen F., Boncio P., Visini F., Pace B., Valentini A., Baize S. & Scotti O. (2020) - Probability of occurrence and displacement regression of distributed surface rupturing for reverse fault. Frontiers in Earth Science, https://doi.org/10.3389/feart.2020.581605.

Oddone E. (1915) - Gli elementi fisici del grande terremoto marsicano-fucense del 13 gennaio 1915. Boll. Soc. Sismol. Ital, 19, 71-215.

Patacca E., Scandone P., Di Luzio E., Cavinato G.P. & Parotto M. (2008) - Structural architecture of the central Apennines: Interpretation of the CROP 11 seismic profile from the Adriatic coast to the orographic divide. Tectonics, 27(3).

Patruno S. & Scisciani V. (2021) - Testing normal fault growth models by seismic stratigraphic architecture: The case of the Pliocene-Quaternary Fucino Basin (Central Apennines, Italy), Basin Research, 33(3), 2118-2156.

Petersen M. D., Dawson T.E., Chen R., Cao T., Wills C.J., Schwartz D.P. & Frankel A.D. (2011) - Fault displacement hazard for strike-slip faults. Bulletin of the Seismological Society of America, 101(2), 805-825.

Reimer P.J., Bard E., Bayliss A., Beck J.W., Blackwell P.G., Ramsey C.B., Buck C.E., Cheng H., Edwards R.L., Friedrich M. & Grootes, P.M. (2013) - IntCal13 and Marine13 radiocarbon age calibration curves 0–50,000 years cal BP. Radiocarbon, 55(4), 1869-1887.

Serva L., Blumetti A.M. & Michetti A.M. (1986) - Gli effetti sul terreno del terremoto del Fucino (13 Gennaio 1915); tentativo di interpretazione della evoluzione tettonica recente di alcune strutture. Mem. Soc. Geol. It., 35(1986), 893-907.

Technical Commission on Seismic Microzonation (2015) - Land Use Guidelines for Areas with Active and Capable Faults (ACF), Conference of the Italian Regions and Autonomous Provinces – Civil Protection Department, Rome, 2015.

Testa A., Valentini A., Boncio P., Pace B., Visini F., Mirabella F. & Pauselli C. (2021) - Probabilistic fault displacement hazard analysis of the Anghiari–Città di Castello normal fault (Italy). Italian Journal of Geosciences, 140(3), 327-346.

Youngs R.R., Arabasz W.J., Anderson R.E., Ramelli A.R., Ake J.P., Slemmons D.B., McCalpin J.P., Doser D.I., Fridrich C.J., Swan III F.H. & Rogers A.M. (2003) - A methodology for probabilistic fault displacement hazard analysis (PFDHA). Earthquake spectra, 19(1), 191-219.